

Chapter 13

Interface with Experimental Detector in the High Luminosity Run

H. Burkhardt^a and F. Sánchez Galán^b

^a*CERN, EP Department, Genève 23, CH-1211, Switzerland*

^b*CERN, BE Department, Genève 23, CH-1211, Switzerland*

We describe the main general changes as relevant for the experiments, and in particular the changes in the machine-detector interface (MDI) region extending from the merging of the LHC beampipes into a single experimental chamber before the inner triplet to the start of the experimental beampipe in the experimental cavern. The geometry of this region is optimized to provide a maximum decoupling of the activities in the tunnel and inside the experimental caverns. Massive absorbers are used to strongly reduce the flux of secondary particles produced in collisions in the interaction region into the tunnel, and at the same time help to protect the experiments from beam induced losses and backgrounds. This chapter explains the main challenges within that region and how they will be solved to cope with the new requirements coming from the luminosity upgrade.

1. Introduction

The machine upgrade for high luminosity requires major changes on the machine side. Key ingredients for the luminosity increase are larger apertures in the focusing sections around the experiments and higher beam intensities.¹

The experiments are upgraded for reduced inner beam pipes with more powerful vertex detectors. This is important for physics and essential for the increased pile-up. Other key design considerations for the upgraded LHC detectors include longevity at increased radiation levels, minimisation of activation and exposure to personnel by remote handling.

This is an open access article published by World Scientific Publishing Company. It is distributed under the terms of the Creative Commons Attribution 4.0 (CC BY) License.

As is often the case in machine-detector interfacing, these are to some extent conflicting requirements, which require a coherent planning for experiments and machine together.

1.1. Overview of the main changes relevant for the experiments

In this chapter, we discuss more generally hardware changes of relevance to the experimental regions, with respect to the original design of the LHC as described in the LHC design report.² The changes required for the high-luminosity upgrade and the requests and planning of the experiments for the future running of the LHC have been discussed in several joint machine-experiments workshops.^{4,5}

Figure 1 shows the schematic layout of the LHC with its four interaction regions.

The HL-LHC design is for four experiments, the two high-luminosity experiments ATLAS and CMS at IR1 and IR5, and the ALICE and LHCb experiments installed at IR2 and IR8.

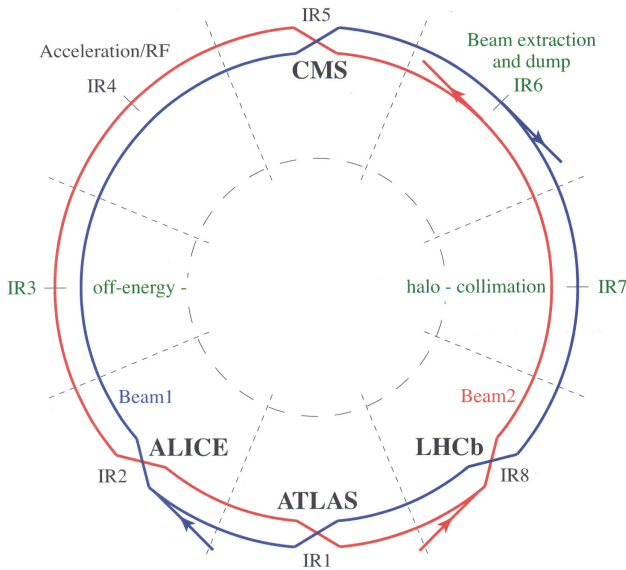


Fig. 1. Schematic layout of the LHC with its four interaction regions which provide collisions to the ALICE, ATLAS, CMS and LHCb experiments.

Table 1. Target luminosities \mathcal{L} for p-p operation for the LHC and HL-LHC. For the HL-LHC, the ATLAS and CMS target luminosities include luminosity leveling which will allow for constant luminosities for the first hours during a fill.

IR	LHC $\mathcal{L}, \text{cm}^{-2}\text{s}^{-1}$	HL-LHC $\mathcal{L}, \text{cm}^{-2}\text{s}^{-1}$	Experiment
1	1×10^{34}	5×10^{34}	ATLAS
2	1×10^{31}	1×10^{31}	ALICE
5	1×10^{34}	5×10^{34}	CMS
8	4×10^{32}	2×10^{33}	LHCb

Table 1 shows the target luminosities for the experiments in proton-proton collisions in the LHC as originally designed, and for the high-luminosity upgrade. The main luminosity upgrade is for the interaction regions IR1 and IR5 and will be implemented in the long shutdown LS3.

The ALICE and LHCb experiments installed in IR2 and IR8 already had significant detector upgrades during LS2 in 2020. LHCb has asked for a luminosity increase to $2 \times 10^{33} \text{cm}^{-2}\text{s}^{-1}$, to be implemented in RUN3. This is possible without major changes to the magnet layout in IR8 and the required detector and vacuum beam pipe upgrades can be implemented in the long shutdown LS2. It is accompanied by an improved shielding (TANb at D2), to minimize the impact of the increase in radiation and heating of cold machine elements. A second upgrade by LHCb targeting luminosities of $1\text{--}2 \times 10^{34} \text{cm}^{-2}\text{s}^{-1}$ after LS4 is currently being studied.^{6,7}

The low target luminosity for ALICE in pp operation requires collisions with large transverse offsets. The future plans for the ALICE pp programme are described in.⁸ The possibility to install an entirely new detector in IR8 in LS4 for heavy ion operation at significantly increase luminosities has been proposed⁹ and is presently under study.

In discussions with all experiments in the HL-LHC coordination working group during 2013, it was confirmed that the LHC machine upgrade design can be considered as dedicated to high-luminosity and should not be constraint by other modes of operation, which can be completed before LS3. High-beta* ($\gg 30 \text{m}$) operation is not planned after LS3. The experimental programs of the smaller dedicated forward experiments (LHCf, TOTEM) requiring special low luminosity LHC operation does not extend beyond LS3. At the same time, there is a general consensus that new ideas to fully exploit the unique physics potential of the HL-LHC without compromising its main goals should always

be welcome. Several smaller new detectors FASER, SND and MoEDAL have been proposed and will likely operate in future LHC runs, mostly in passive, parasitic mode.^{10–12}

From year 2016 in RUN2, forward detectors (Roman Pots) were successfully used in standard physics to tag forward protons at distances of 220–240 m from IP1 and IP5.¹⁴ TOTEM has now been integrated into the CMS collaboration, and expressed a strong interest for a continued operation of roman pot detectors in the space available near Q6 and possibly 420 m in standard HL-LHC runs.¹³

The magnet layout in IR1 and IR5 will change significantly. This is shown schematically in Figure 2 for the first 80 m from the interaction point and discussed in detail in the following Chapter.¹⁵ The distance of the first quadrupole magnet (Q1) from the IP will remain the same (23 m) as before the upgrade.

The most relevant machine modification for the experiments will be the installation of the new large aperture triplet magnets Q1-Q3 in IR1 and IR5. The inner coil diameter of these triplet magnets will increase by roughly a factor of two from 70 mm to 150 mm.

As presently the case, the magnet layout will be the same for IR1 and IR5, and also remain approximately left/right anti-symmetric with respect to the interaction points.

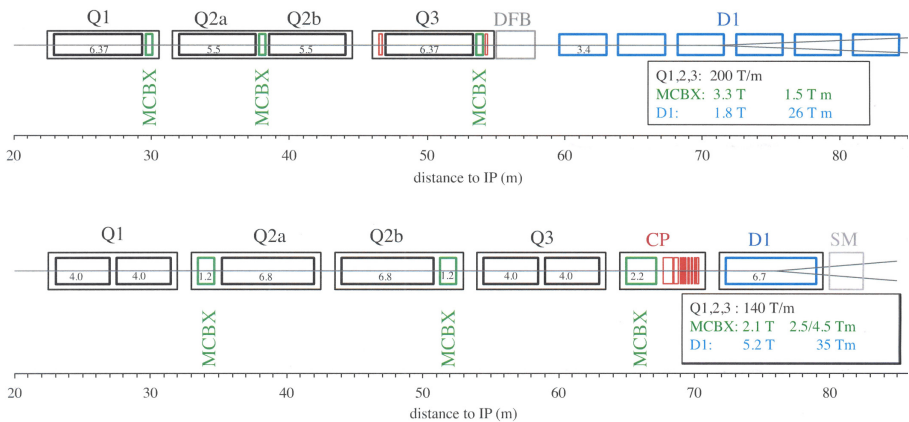


Fig. 2. Schematic magnet layout for the current LHC (top) and the HL-LHC in IR1 and IR5 (bottom) up to first separation magnet D1.

2. Experimental Beam-pipes

The four large experiments have asked for reductions of the diameter of the central beam pipes. Table 2 summarizes the original and reduced inner beam pipe radii. For ATLAS and CMS the new reduced aperture beam pipes were installed during LS1 and successfully used in LHC RUN2. The LHCb VELO¹⁶ is movable. It is only closed in stable physics to the value shown in the table, and retracted to 30 mm otherwise. Based on aperture studies, the good experience in RUN2 and detailed simulations including failure scenarios, it was agreed that the reduced central chamber sizes can be kept for HL-LHC. A further decrease from 19 mm to 16.5 mm radius for the central piece of the ALICE beam pipe over 500 mm length has been requested for LS3 and is currently under study.

Table 2. Original and reduced inner beam pipe radii at the IPs.

IP	original r_{\min} mm	reduced r_{\min} mm	Experiment	when
1	29	23.5	ATLAS	LS1
2	29	19	ALICE	LS2
5	29	21.7	CMS	LS1
8	5	3.5	LHCb, VELO	LS2

3. Failure Scenarios and Experiments Protection

Active machine protection, based on continuous beam loss monitoring (BLM) and fast beam dump (within 3 turns) has already been proven to be essential and reliable for the present LHC. It will be even more important for the HL-LHC. In addition to the protection of the machine elements described in Chapter 12,¹⁷ we will have to rely on active protection for the experiments. This implies, that we have to identify all relevant failure scenarios which may result in significant beam losses to the experiments, and to make sure that these abnormal beam losses can be detected sufficiently fast and beams be dumped before they cause any significant damage to the experiments.

Detailed studies with particle tracking have been performed for the HL-LHC. Most critical for experiments protection is the operation at top energy with squeezed beams. The potentially most relevant failures scenarios for the HL-LHC are:

- Asynchronous beam dumps¹⁸
- Crab cavity failures¹⁹
- Mechanical non-conformities, i.e. objects which accidentally reduce the aperture (example RF-fingers) or UFO's (dust particles falling through the beam) resulting in showers with local production of off-momentum and neutral particles around the experiments.²⁰

Other more or less dangerous scenarios do exist but are not expected to pose significant extra risks to the experiments, not covered by the machine protection and fast dump systems. These include:

- D1 magnet failures. The present 6 warm D1 magnets at either side of IP1 and IP5 will be replaced with single superconducting D1 magnets with longer time constants well within the capabilities of the machine protection.
- Injection (kicker) failures and grazing beam impact on injection elements (TDI).

The injection and dumping systems are described in Chapter 19.²¹

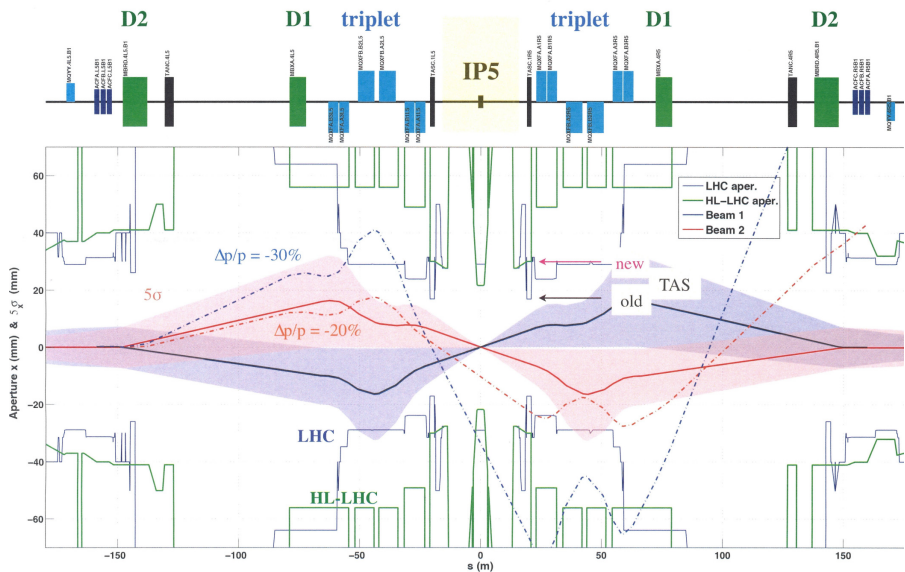


Fig. 3. Schematic view of IR5 with beam envelopes and apertures.

Figure 3 shows a schematic view of IR5 with beam envelopes and apertures. Beam-pipe apertures are shown as lines as implemented in present simulations, both for the LHC as originally build for RUN1 (dark blue lines), as well as for the HL-LHC after LS3 (green). The coloured bands show 5σ beam envelopes for $\beta^* = 15$ cm as relevant for the HL-LHC. Two off momentum tracks with $\Delta p/p = -20\%$ and -30% are also shown. A -30% track originating at 150 m from the interaction point (originating by collisions of beam particles with dust particles, for example) will pass through the enlarged HL-LHC apertures and directly hit the central experimental beam pipe.

Figure 4 illustrates the beam envelope growth induced by an immediate 90° phase jump on a single crab cavity.

High amplitude particles are removed in the LHC by the collimation system in dedicated cleaning sections far from the experiments.²² The experience in LHC RUN1 and RUN2 and detailed simulations have shown that the LHC collimation and machine protection systema are very effective to protect the machine and experiments from uncontrolled beam losses, but also require a continuous follow up of safety considerations and safe operational procedures.

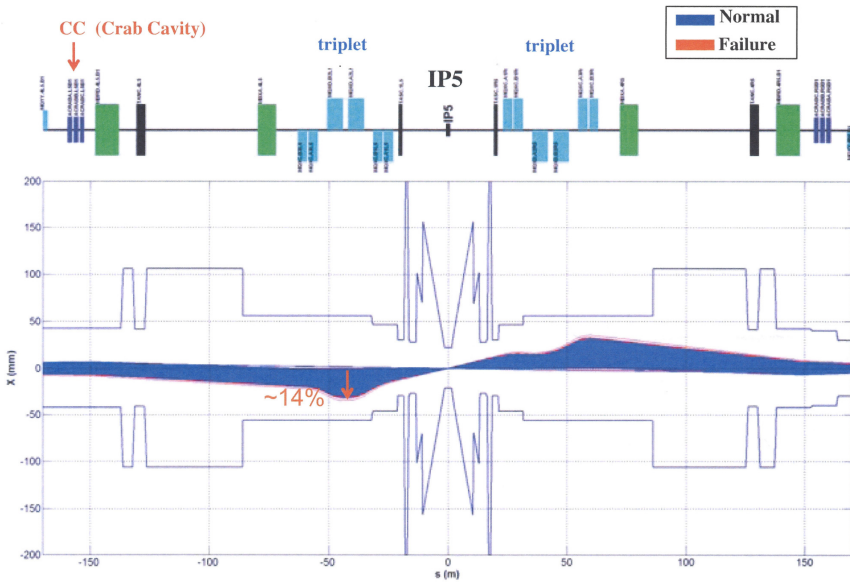


Fig. 4. Schematic view the beam envelope growth induced by a crab-cavity failure, resulting in a growth of 14% within 5 turns.

4. Machine Induced Backgrounds

Machine induced backgrounds in the LHC are generally dominated by beam gas scattering. Beam gas backgrounds scale with the beam intensity and vacuum pressure and are to a large extent generated locally in the straight section and dispersion suppressors around the experiments. Under normal conditions, they depend only weakly on optics details and collimator settings.

Background conditions have generally been very good in RUN1 and RUN2 of the LHC.²³ Signal to background ratios of the order of 10^4 were observed in good running conditions in ATLAS and CMS.

For ALICE, which operates at much lower luminosity, machine induced backgrounds are more critical. Excellent vacuum conditions (pressures below 5×10^{-9} mbar) are essential for ALICE. During part of the proton-proton operation in 2012, machine induced backgrounds in ALICE were too high to permit data taking. This was related to heating in the injection absorber (TDI) region and has already been improved for RUN2 and is not expected to cause problems for the upgraded injection and vacuum systems relevant for HL-LHC.

Continued efforts to monitor, understand and minimise backgrounds are important for all experiments. Increases in intensity and luminosity generally translate also in more heating, out-gassing and potentially increased backgrounds. There have already been major changes in running conditions in the LHC between RUN1 and RUN2. Potential reasons for an increase of backgrounds between RUN1 and RUN2 were:

- more synchrotron radiation, by the increase of beam energy from 4 to 6.5 TeV at beginning of RUN2
- electron cloud due to reduced bunch spacing, main step 50 ns \rightarrow 25 ns at beginning of RUN2
- electron cloud due to increased bunch intensities
- local heating from increased intensities.

While these effects were in fact observed, their effect was largely mitigated by many improvements on hardware and also generally improved understanding and control of the LHC, such that backgrounds in LHC2 were not an issue and in some case even better than in RUN1 (in particular for ALICE). Towards the end of RUN2, there have been first signs of a possible background

increase induced by losses on tertiary collimators for operation at low β^* . This is at present followed up by simulations comparing both LHC and HL-LHC conditions and benchmarking with the RUN2 observations of the LHC experiments, with the aim to assure that the background conditions for the experiments remain excellent also for HL-LHC.

5. Engineering Challenges

As explained in the previous sections, the luminosity reach of ATLAS and LHC at the HL-LHC era implies new constraints for the protection of the inner triplets from the machine debris. One of the most challenging comes from the fact that activation levels will increase a factor of 15–30 from the 2015 values (LS1), affecting both radiation tolerance of equipment and the ability to perform routine maintenance operations. Figure 5 shows the residual dose rates at a standard working distance in the tunnel.²⁴

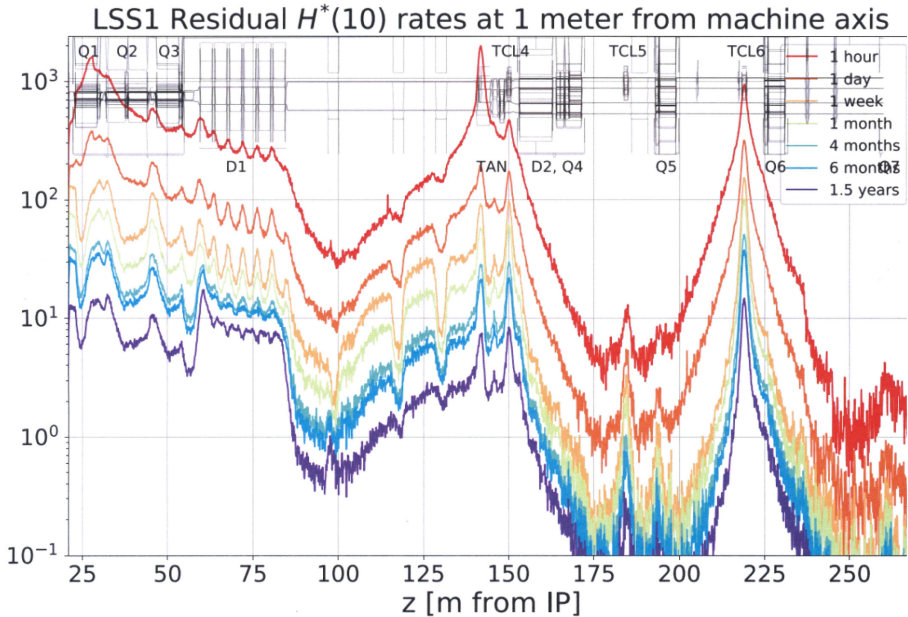


Fig. 5. Point 1 summary 1D profile of residual dose rates at 1 meter distance from beam axis, on average 40cm from outer surface of cryostats. Cooling times referenced to end of Run 3 p-p operations.

When the Proton (or ion) bunches traveling in opposite directions traverse each other at the interaction points there is a probability that two or more particles will come close enough to interact. The event generates a number of high-energy collision products, some having an electric charge (like pions+/-, protons, etc.), other being neutral (like neutrons, gammas etc.). Some of these particles leaving the IP could impinge on the front face of the inner triplet superconducting quadrupole Q1 or the superconducting dipole D2 situated in front of the vacuum recombination chamber producing a quench.

For the LHC, special purpose absorbers called TAS and TAN stop these secondary particles and concentrate the radiation, allowing a safe operation of Q1 and D2. At the same time, due to the proximity to the interaction region, ($22.1\text{m} < z$) the TAS absorbers are surrounded by a massive shielding to reduce the background radiation in the detectors generated by the interactions taking place in the TAS. In this way, TAS absorber and its surrounding are a highly radioactive environment and form an integral part of the forward shielding of both ATLAS and CMS.

The design of the upgraded TAS and TAN (namely TAXS and TAXN) and new equipment takes into account additional challenges, as the increased energy deposition, alignment capabilities and the radiation constraints and in consequence, the entire layout of tunnel equipment near the interaction regions (machine-interface region) will allow for simplified maintenance.³

The typical machine-interface region is a dead-end region extending from the end of the inner triplet Q1 to the start of the TAS ($20.8 < z < 22.1\text{m}$). Due to the shielding requirements, the access to that area is very narrow (40 cm wide passage for personnel from the tunnel wall to the elements belonging to the LHC machine and auxiliary beam line equipment's), and the space surrounding is limited in all directions. Furthermore, only 1.3 m are available longitudinally to house multiple equipment essential for operation:

- a Helium tightness dome (which secures the close region in the experimental area in case of Helium release from the triplet)
- a Beam Positioning Monitor (BPM)
- two all-metal gate vacuum valves
- a module containing a residual gas analyser + ion pump + Non-Evaporable Getter (NEG) cartridge + diverse gauges Bayard Alpert, Penning and Pirani gauges (“VAX module”)

- bellows
- services ancillaries (piping and cabling).

Routine operations of elements like the BPM's (i.e. alignment) are very difficult to perform and equipment replacement in case of failures needs to be done manually by a single person, without the possibility of lifting systems. The confined space presents also a safety risk in case of an evacuation or an intervention by the fire brigade.

6. Relocation of Vacuum Experimental Modules (VAX)

As indicated previously, multiple studies about the residual dose rates in the whole LHC machine, and in particular both in ATLAS and CMS show that the values following HL-LHC operation (3000/fb) are likely increasing by a factor which is consistently between 15 and 30 times the values measured in the First Long Shutdown (LS1).²⁴ This is of key importance for the regions close to the TAS, as there is little room to improve the current situation: No modifications of the massive steel and concrete shielding (which tightly surround the equipment) are possible, and also alignment requirements for the last BPM will now become critical for operation, thus requiring more frequent survey interventions.²⁵

The design of new equipment takes into account these constraints and the equipment in the machine-experiment cavern boundaries will be optimised for simplified maintenance. In this way, the new design focused on the use of reduced activation materials and improving (reducing time and avoiding contact during handling) or eliminating the need of interventions. Nevertheless, there is little room to improve the accessibility to the subsystems in the Q1-TAS region, as in HL-LHC will still be an extremely narrow dead-end zone where no modifications of the massive steel and concrete shielding (which tightly surround the equipment) are possible.

The situation could be substantially improved by relocating the equipment to the other side of the TAS (from the tunnel to the inside of the experimental caverns), where the massive existing forward shielding structures would have to be slightly modified, however with a negligible loss of performance for background shielding. The available "empty" space in that region is also limited during operation, but at every yearly-programmed shutdown, the massive steel shielding structures are dismantled or opened to free up space, allowing the

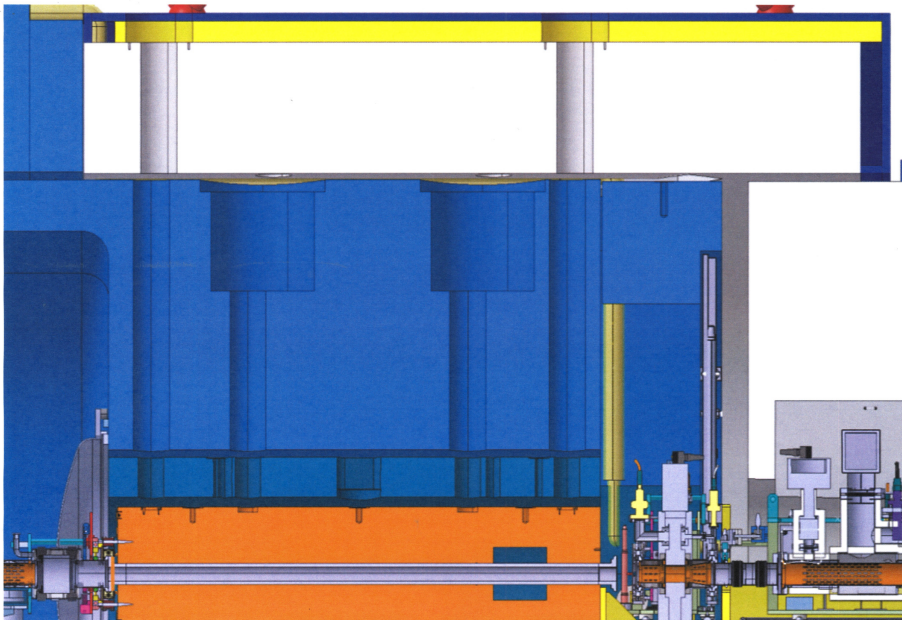


Fig. 6. 2D view of the ATLAS machine-experiment interface region, with the TAXS (orange) inside the blue, TX1S fixed steel shielding. Experimental cavern is on the right, the relocated VAX is inside the white ATLAS Forward mobile shieldings.

detectors to be opened. In this way, after the removal of the forward shielding structures, access is easier than in the tunnel and the intervention doses can be drastically reduced with the use of remote handling and keeping a much safer distance respect to the one existing at the tunnel side.

The proposed relocation requires modifications in the forward shielding regions of ATLAS and CMS to host the support and the modules while being compatible with the standard opening scenarios.

The proposal for HL-LHC started revising the need of each equipment and services. The exercise resulted first in the integration of the element requiring more interventions, the BPM within Q1 (being in secondary vacuum improves reliability, and eliminates the need of independent alignment), and second the installation of a new-cantilevered support in the experimental cavern, which includes guiding columns and self-plug-in connectors hosting both electrical and pneumatic lines. The equipment will be remotely handled and automatically plugged-onto the supports with the use of a robot attached to



Fig. 7. The CERN CRANEbot is seen here carrying a VAX module (centre of the image) inside the CMS cavern, as part of an operation test conducted in early February 2021.

the the cranes situated at the experimental caverns. An intense validation campaign followed by a successful proof of principle test in CMS cavern was performed in LS2. During the test in the CMS cavern, the robot, handled by a crane, was remotely operated to locate the VAX module on its place in the support and then uninstall it. The robot was able to grab and release the lifting rings as well as to assist in the alignment operation on the guide pins in order to correctly reach the support.

The proposed modifications in shielding structures inside the experimental caverns were advanced to LS2, where a number of subsystems were modified (in ATLAS: JTT, JFC1, JFC2, JFC3, VT chamber supports and in CMS: beampipe support and shielding inserts) and will be completed during LS3.

7. Secondaries Absorbers for HL-LHC, TAXS

The Target Absorbers for charged Secondaries and Neutral particles TAS and TAN of the present LHC will be replaced in LS3 by modified, larger aperture

absorbers referred to as TAXS and TAXN and in LS2 a new Target Absorber for Neutrals was installed at both sides of LHCb (IR8).

The high-luminosity interaction regions IR1 and IR5 of the present LHC are equipped with 1.8 m long copper absorbers called TAS at 19 m from the interaction points, located in front (IP side) of the first superconducting quadrupoles Q1, see Figure 8.

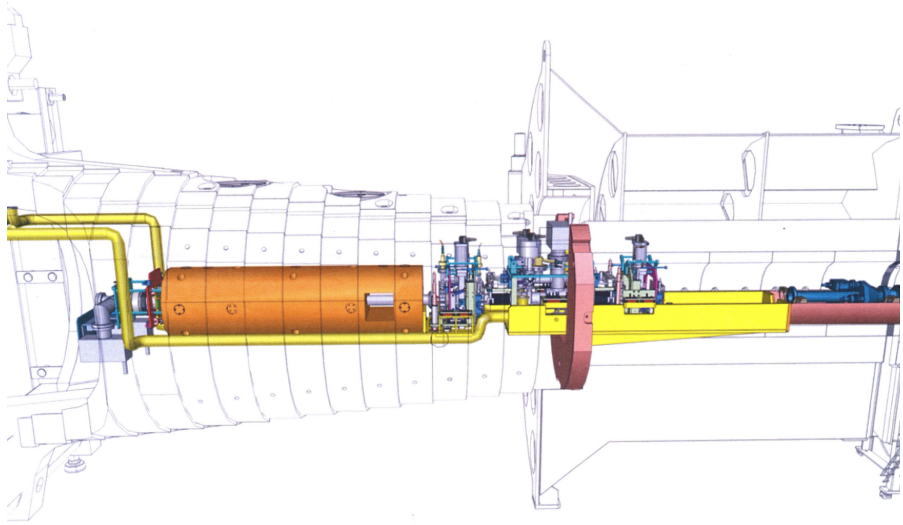


Fig. 8. 2D Layout drawing showing left side of IR5 (CMS). The TAXS (orange) is surrounded by the FIN shielding. IP is at the right, while the relocated VAX can be seen at the right of it, at the experimental side).

Their primary function is to reduce the energy flow from collision debris into the superconducting quadrupole triplet magnets. In addition, the TAS also acts as a passive protection. It reduces the flux of particles into the inner detectors of ATLAS and CMS in case of abnormal beam losses. The inner radius of the TAS as presently installed is 17 mm both in IR1 and IR5. This is significantly less than the central beam pipe radius of ATLAS and CMS. The radius of the reduced central beam pipes installed in LS1 was chosen such, that they still remain in the shadow of the TAS, including alignment tolerances and sagging. This is of direct relevance for high- β^* operation in the LHC, where the beam size is approximately constant throughout the experimental regions.

For the HL-LHC upgrade, the inner coil diameter of the triplet magnets will increase from 70 mm to 150 mm. The inner radius of the present TAS will also increase from 17 to 30 mm for the TAXS, which will be significantly larger than the radius of the central beam pipes. The material (Cu), length and outer dimensions remain as originally designed. Additional shielding will be installed around the beam screens in the triplet region. The energy deposition for the enlarged beampipe inside the TAXS to the triplet magnets has been determined by simulations and remains within specifications, see Chapter 10. The absorbed power will increase imposing an active cooling to have a TAXS compatible with beam operating temperatures.

Understanding, minimising and mitigating any un-avoidable negative impact of the machine upgrade to the experiments is a key objective of the machine detector interface for the HL-LHC.⁴ Increasing the central beam-pipes after LS3 in the same proportion as the inner TAS radius would compromise the vertex detector performance. Optimal vertex resolution for ATLAS and CMS is essential to deal with the increased pile-up after LS3. The beam pipe radii in the central detector region will remain after LS3 at the reduced values given in Table 2. Detailed tracking studies including failure scenarios further described in¹⁷ have shown that the experiments remain well protected in case of accidental beam losses in spite of increased intensities and apertures.

8. Neutral Absorbers for HL-LHC (TAXN, TANB)

There will also be major changes further outside in IR1 and IR5. The D2 magnet and neutral absorber TAN which is located in front of the D2 magnet will move by 13 m closer to the interaction points, to make space available for the installation of the crab cavities. The β -functions at the TAN will increase and require a larger aperture of the vacuum recombination chamber (Y-chamber) inside the TAN. The half-crossing angle will roughly double for the HL-LHC (from typically 142.5 to 295 μ rad) and move the neutral cone from collision debris closer to the beam aperture of the TAN. The TAN surrounds both beams and also acts as passive absorber for the incoming beam. Similar to the TAXS, energy deposited will increase in the TAXN, making an active cooling compulsory. The increase in aperture results in a reduction of passive protection compared to the present LHC, which will be minimised by closer matching of the holes through the new TAXN to the beam geometry and by addition of movable collimators.

The LHC luminosity upgrade of the LHCb detector located at the Interaction Point 8 (IP8) will also represent an increase of the inelastic collisions. Same as for IP1 and IP5, The pp collisions will produce a shower of forward particles, namely of neutrals (mostly neutrons and photons) and charged particles (mostly pions and protons), that will leave the interaction point 8 in both directions towards the machine creating a non-negligible energy deposition in the region. With these conditions and without the use of an absorber, the D2 recombination dipoles will see an energy deposition that could bring them above their safety thresholds risking quenching. For protecting these dipoles, a minimal absorber TANB (shown in Figure 15) was installed on either side of IP8 to reduce the heat load on the D2 magnets to values well below the quench level.

Four TAXN neutral particle absorbers will be installed in LS3, each unit around 125 m away on each side of IP1 and IP5. Same as for the replaced TANs, their initial goal is to protect the separation dipoles D2 and the quadrupoles of the Matching Section from the power carried off by neutrals produced at the interaction point. They will host detectors inside to study the very forward physics and to measure the relative and absolute luminosity.

The TAXNs located around IP1 and IP5 will be instrumented with the machine beam rate monitor (BRAN) and the Zero Degree Calorimeter (ZDC). Each detector is considered as a separate ‘small experiment’ to be integrated and installed inside the TAXN in the LHC tunnel.

The TAXNs, shown in Figure 9, are 30 tonne absorbers composed by 9 subassemblies. Positioned with customised pins, each subassembly is below 5 tonne in weight. The stainless steel recombination vacuum chamber is at the centre of the Absorber Box, the inner assembly of a TAXN, and it is clamped inside the two water-cooled absorber clam shells. This 4.3 m long vacuum beam chamber has a large tube facing the interaction point which transitions smoothly into two tubes going away from the IP. Both, the copper absorber and the chamber, are surrounded by heating jackets for bake-out purposes. An assembly composed of Five carbon steel (St-36) blocks surround the Absorber Box for radiation protection purposes: two Base Plates (Lower and Upper), two Lateral Shieldings and the Top Shielding. Two marble blocks are located on the IP end providing a personnel lower radiation area inside the Long Straight Section. Finally, the complete assembly is supported by three jacks which can be remote aligned to optimise the recombination chamber aperture.

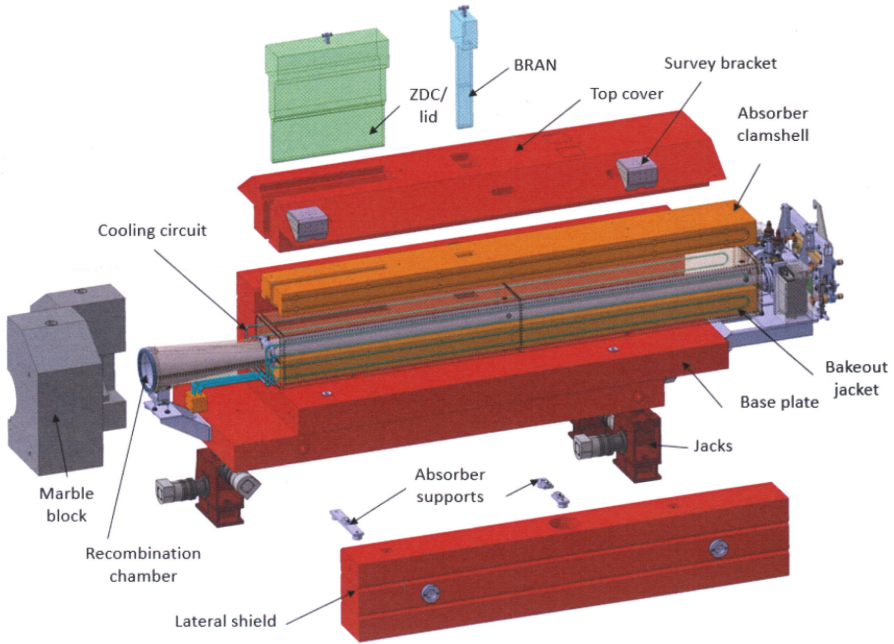


Fig. 9. TAXN developed overview. Detectors geometries represent exclusively a space reservation.

There are two open slots inside the TAXN which are accessible from the top and that will host the Luminosity and Forward Physics detectors. The BRAN is foreseen to remain installed during the complete LHC run, and the ZDC, which will be in place only during the Pb-Pb run. For this reason, a lid covers the ZDC slot during the proton-proton run providing radiation protection to personnel and equipment.

The main constraints and functionalities with which the design shall comply are:

- The heat loads from IP collision debris. The energy deposition mainly comes from neutral particles impacting the absorber block resulting in a highly peaked profile as is shown in Figure 10.
- The length of the absorber as well as the beam pipe separation of the recombination chamber allow protecting the downstream magnets from collision debris while the surrounding elements (i.e. collimators) receive a heat load that can be extracted by their cooling system.

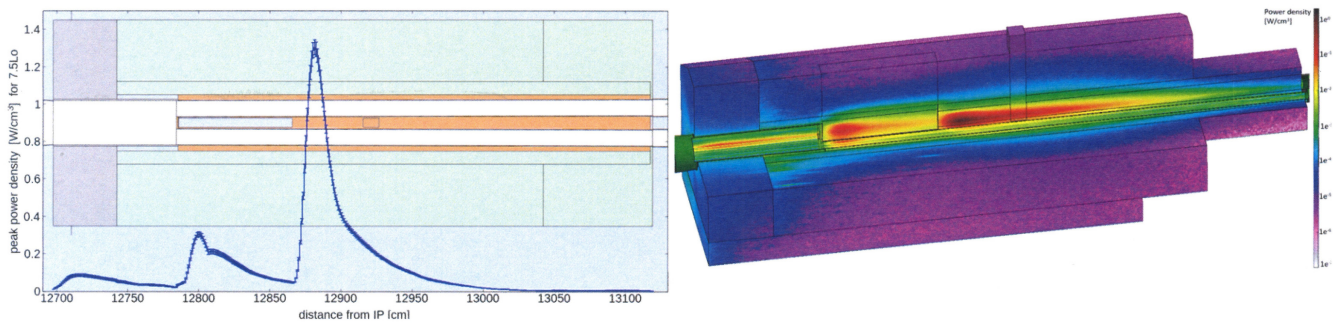


Fig. 10. Left: 2D plot of TAXN showing the heat deposition peak distribution along the beam machine axis. Right: 3D cut view showing the heat deposition distribution along the transverse plane.

- The integration of the bakeout system required to achieve the foreseen vacuum conditions for the operation of the LHC machine.
- The transverse beam aperture and impedance limits for the LHC proton and Pb-Pb beam. The beam aperture for the HL-LHC layout v1.5 flat optics at 14σ is shown in Figures 11, 12 and 13. The 12.5σ expected in the inner triplet and dipole 1 showing that there is a margin of 1.5σ in terms of aperture.
- The high expected radioactive environment.

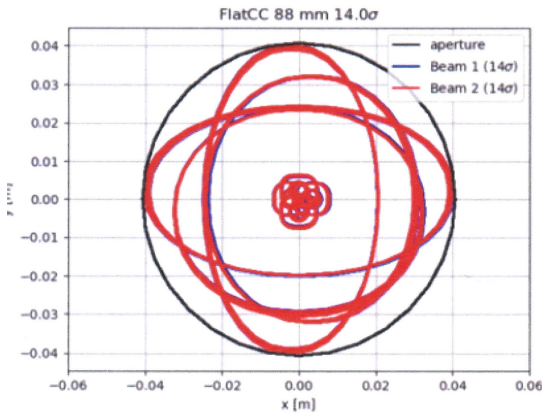


Fig. 11. Vertical transverse cross-section.

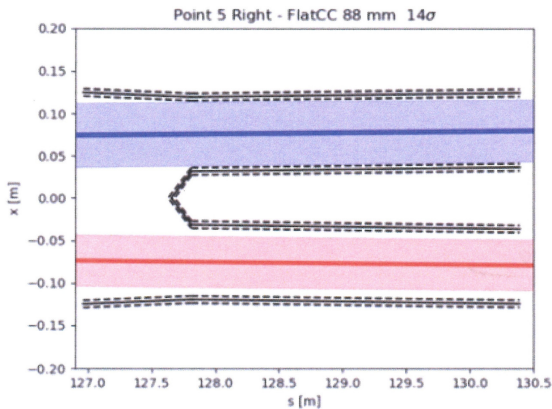


Fig. 12. Longitudinal horizontal cross section.

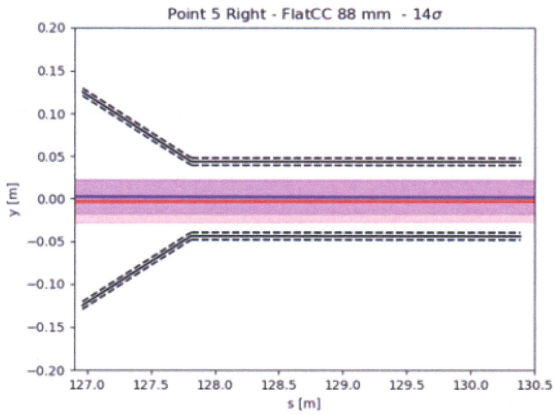


Fig. 13. Longitudinal vertical cross section.

- The alignment system of the TAXN itself and its neighbours components.
- The integration of the ZDC and BRAN detectors to provide an optimised environment for the full exploitation of their physics case and functionalities (ion or p-p runs).
- The LHC operation and tunnel integration as shown in Figure 14.

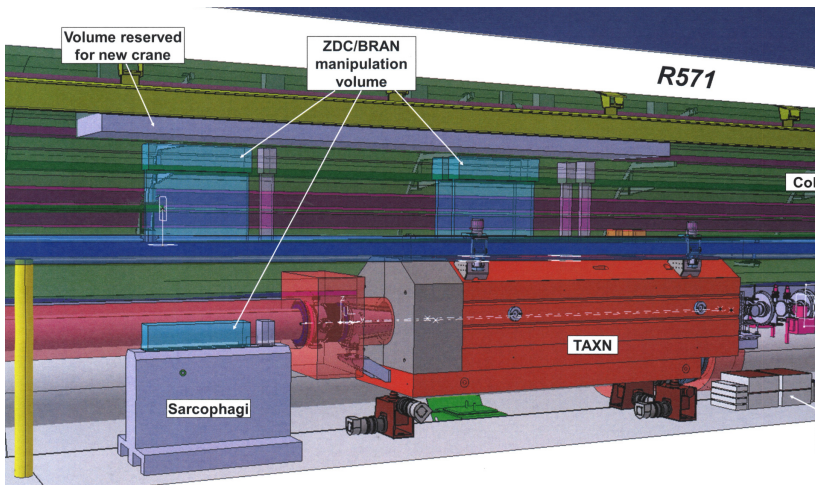


Fig. 14. TAXN integration inside the LHC tunnel.

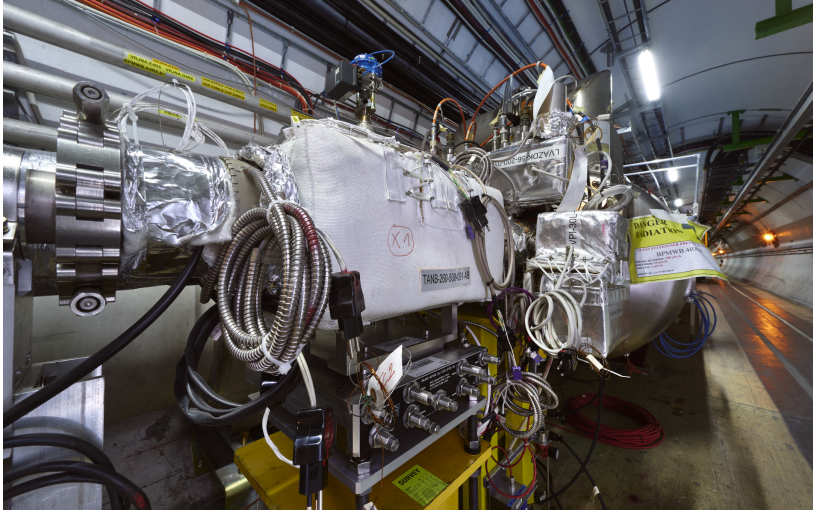


Fig. 15. The TANB absorbers were installed in the LHC tunnel to protect the accelerator components from particles produced by collisions occurring in the LHCb experiment. The alignment table can be seen below the absorber.

Similar as in IP1 and IP5, the luminosity increase require a new absorber at IR8, to protect the superconducting dipole D2, although energy deposition levels and integration constraints led to a different design without surrounding the vacuum recombination chamber. The TANB (shown after installation in Figure 15) is composed by two blocks of high density material (in this case tungsten) clamping the two beam chambers approximately 1.9m before D2 towards the IP8, on either side of IP8, creating a static mask to stop the forward neutral particles while letting the beam inside the vacuum chambers pass by undisturbed.

The continuous deposition during HL-LHC operation will activate the TANB, limiting any human activity in the region to very strict access and short time periods. Among these activities, alignment is placed as one of the most time consuming and one that obliges a closer proximity with the TANB absorber mainly due to the current design of the “standard” CERN alignment platforms. This will be much improved from LS2 as, following the ALARA (As Low As Reasonably Achievable) approach, a new alignment platform was engineered. The new alignment plate is based upon the design of the “standard” CERN alignment platforms, moving the actuators for each

degree of freedom to a single side (in this case, the transport side of the tunnel) facilitating its access, improving the ergonomics of the alignment operations and principally decreasing the time and proximity from the operator to the equipment mitigating the exposure of the professionals to the activated area.

References

1. Rossi, Lucio (ed.) (CERN); Brüning, Oliver (ed.) (CERN), “The High Luminosity Large Hadron Collider: the new machine for illuminating the mysteries of Universe”, Hackensack, NJ: World Scientific, 2015.
2. O. Brüning et al. (ed.), LHC design report. Vol. 1-3, CERN-2004-003-V-1–3.
3. Apollinari G. (ed.) (FERMILAB); Béjar Alonso I. (ed.) (CERN); Brüning O. (ed.) (CERN); Fessia P. (ed.) (CERN); Lamont M. (ed.) (CERN); Rossi L. (ed.) (CERN); Tavian L. (ed.) (CERN), “High-Luminosity Large Hadron Collider (HL-LHC): Technical Design Report V. 0.1”, CERN Yellow Reports: Monographs.
4. H. Burkhardt, D. Lacarrere, L. Rossi, Executive summary of the 1st Collider-Experiments Interface Workshop on 30 Nov. 2012.
5. ECFA High Luminosity LHC Experiments Workshop, Aix-Les-Bains, 3-6 Oct. 2016.
6. LHCb Collaboration, “Expression of Interest for a Phase-II LHCb Upgrade: Opportunities in flavour physics, and beyond, in the HL-LHC era”, CERN-LHCC-2017-003.
7. I. Efthymiopoulos et al., LHCb Upgrades and operation at $10^{34} \text{ cm}^{-2} \text{ s}^{-1}$ luminosity – first study, CERN-ACC-NOTE-2018-0038.
8. ALICE collaboration, “Future high-energy pp programme with ALICE”, ALICE-PUBLIC-2020-005.
9. D. Adamova et al., “A next-generation LHC heavy-ion experiment”, <https://arxiv.org/abs/1902.01211v2>.
10. A. Ariga et al., “Technical proposal: FASER, The forward search experiment at the LHC” CERN-LHCC-2018-036
“Detecting and Studying High-Energy Collider Neutrinos with FASER at the LHC”, CERN-LHCC-2019-012.
11. C. Ahdida et al., “SND@LHC - Scattering and Neutrino Detector at the LHC”, CERN-LHCC-2021-003.
12. B. Acharya et al., “MoEDAL Run-3 Technical Proposal”, CERN-LHCC-2021-006.
13. M. Albrow et al., “CMS-TOTEM Precision Proton Spectrometers CT-PPS”, CERN-LHCC-2014-021.
14. S. Grinstein, “The ATLAS Forward Proton Detector (AFP)”, Nucl. Part. Phys. Proc. 273-275 (2016) 1180-1184.
15. E. Todesco, “Insertion Magnets”, Chapter 6 of this book.
16. LHCb collaboration, “LHCb VELO Upgrade Technical Design Report”, CERN-LHCC-2013-021.
17. D. Wollmann, “Machine protection”, Chapter 12 of this book.

18. A. Tsinganis et al., “Impact on the HL-LHC Triplet Region and Experiments From Asynchronous Beam Dumps on Tertiary Collimators” Proc. IPAC 2017.
19. B. Lindstrom et al., “Crab Cavity Failures Combined with a Loss of the Beam-Beam Kick in the High Luminosity LHC”, Proc. IPAC 2018.
20. Tobias Baer, “Very fast Losses of the Circulating LHC Beam, their Mitigation and Machine Protection”, CERN-THESIS-2013-233.
21. C. Bracco, “Injection and Dumping Systems”, Chapter 19 of this book.
22. S. Redaelli, “Collimation System”, Chapter 8 of this book.
23. LHC Background Study group, <http://cern.ch/lbs>.
24. D. Bjorkman, A. Infantino, “Radiation Protection estimates for LS3 activities in LHC LSS1 and LSS5”, CERN-EDMS2435122.
25. F. Sanchez Galan et al., “Optimising machine-experiment interventions in HL-LHC”, IPAC 2017, Copenhagen.